

Characterization of hyaluronan cable structure and function in renal proximal tubular epithelial cells

W Selbi¹, CA de la Motte², VC Hascall³, AJ Day⁴, T Bowen¹ and AO Phillips¹

¹Institute of Nephrology, Cardiff University School of Medicine, Cardiff University, Cardiff, Wales, UK; ²Department of Immunology, The Cleveland Clinic Foundation, Cleveland, Ohio, USA; ³Department of Biomedical Engineering, The Cleveland Clinic Foundation, Cleveland, Ohio, USA and ⁴MRC, Immunochemistry Unit, Department of Biochemistry, University of Oxford, Oxford, UK

Alteration in the glycosaminoglycan hyaluronan (HA) has been demonstrated in numerous renal diseases. We have demonstrated that renal proximal tubular epithelial cells (PTCs) surround themselves *in vitro* with HA in an organized pericellular matrix or 'coat', which is associated with cell migration, and also form pericellular HA cable-like structures which modulate PTC-mononuclear leukocytes interactions. The aim of this study was to characterize potential regulatory mechanism in the assembly of PTC-HA into pericellular cables. HA cables are generated by PTCs in the absence of serum. Immunohistochemical analysis demonstrates the incorporation of components of the inter- α -inhibitor (I α I) family of proteins and versican into HA cables. Addition of an antibody to I α I/P α I (pre- α -inhibitor) inhibits cable formation. In contrast, inhibition of tumor necrosis factor- α -stimulated gene 6 (TSG-6) has no effect on cable formation, suggesting that their generation is independent of the known heavy-chain transfer activity of TSG-6. Overexpression of HAS3 is associated with induction of HA cable formation, and also increased incorporation of HA into pericellular coats. Functionally, this resulted in enhanced HA-dependent monocyte binding and cell migration, respectively. Cell surface expression of CD44 and trypsin-released cell-associated HA were increased in HAS3-overexpressing cells. In addition, hyaluronidase (hyal1 and hyal2) and bikunin mRNA expression were increased, whereas P α I HC3 mRNA expression was unchanged in the transfected cells. The data demonstrate the importance of I α I/P α I in cable formation and suggest that expression of HAS3 may be critical for HA cable assembly.

Kidney International (2006) **70**, 1287–1295. doi:10.1038/sj.ki.5001760; published online 9 August 2006

KEYWORDS: hyaluronan; cables; TSG-6; HAS; I α I

Hyaluronan (HA) is a ubiquitous connective tissue glycosaminoglycan, which *in vivo* is present as a high molecular mass component of most extracellular matrices. Although not a component of the healthy renal corticointerstitium,¹ increased generation of HA, predominantly in a peritubular distribution, has been demonstrated in both acute and chronic renal injury.^{2–5} The functional significance of alterations in HA synthesis in the renal tubulointerstitium remains unclear.

Exogenous HA, through engagement with its principle receptor CD44, increases migration.⁶ In addition, HA antagonizes the effects of the profibrotic cytokine transforming growth factor- β 1 (TGF- β 1),⁷ by sequestration of TGF- β receptors into lipid raft/caveolin membrane fractions,⁸ which is associated with increased receptor turnover.⁹ HA is not only seen in a soluble extracellular form, but is also assembled into pericellular structures that are associated directly with the cell surface. In proximal tubular epithelial cells (PTCs), this may take one of the two forms: diffuse pericellular 'coats' and HA-based cable-like structures.¹⁰

The wide range of biological actions of HA derives in part from interactions with a wide number of HA-binding proteins, termed hyaladherins. We postulate that the hyaladherins of the inter- α -inhibitor (I α I) family of serum proteoglycans (I α I) and protein product of tumor necrosis factor- α -stimulated gene 6 (TSG-6) are critical to the organization of pericellular HA-based structures. The I α I family includes four plasma proteins, free bikunin, I α I, pre- α -inhibitor (P α I) and inter- α -like inhibitor (I α LI).¹¹ Each of the last three macromolecules exists as a distinct assembly of one bikunin chain and an attached covalently bound unique heavy chains (HCs) (designated HC1, HC2, and HC3). Although the components of the I α I family are synthesized predominantly in hepatocytes, we have previously demonstrated that PTC generate the P α I variant of the I α I family.¹² Much of the work on the associations of I α I-related proteins with extracellular matrix has been carried out in studies of the cumulus cell-oocyte complexes,¹³ where covalent linkage of HCs of I α I (HC1 and HC2) and P α I (HC3) to HA has been demonstrated,^{14,15} which contribute to the stabilization of the extracellular matrix.^{16,17} TSG-6 is also involved in extracellular matrix remodelling.^{18,19} TSG-6 binds HA

Correspondence: AO Phillips, Institute of Nephrology, Cardiff University School of Medicine, Cardiff University, Heath Park, Cardiff CF14 4XN, Wales, UK. E-mail: phillipsao@cf.ac.uk

Received 17 May 2006; revised 21 June 2006; accepted 27 June 2006; published online 9 August 2006

directly and also supports the covalent transfer of HCs of I α I family members to HA, both of which are likely to stabilize HA matrices.

PTCs are known to express two isoforms of human HA synthase (HAS), HAS2 and HAS3. Stimulation of HA synthesis is associated with transcriptional activation of HA synthase 2 (HAS2),²⁰ whereas HAS3 mRNA is constitutively expressed. Overexpression of HAS2, although increasing pericellular HA coats, does not increase cable formation.²¹ Our current study characterizes PTC cables, and in particular the role of HA-binding proteins (hyaladherins) in their formation and function. In addition, by generation of a stable cell line overexpressing HAS3 mRNA, we characterized the role of this HAS isoform in cable generation.

RESULTS

Characterization of HA cables in HK2 cells

Visualization of HA. Photomicrographs of fixed growth-arrested HK2 cells demonstrated diffusely arranged pericellular HA coats over the cell surface as well as in cable-like structures that spanned several cell lengths (Figure 1a), as described previously.¹⁰ Culture of HK2 cells in the presence of fetal calf serum (FCS) increased the number of HA cables on the cell surface (Figure 1b). Limited hyaluronidase digestion removed both the pericellular coats and cables (Figure 1c).

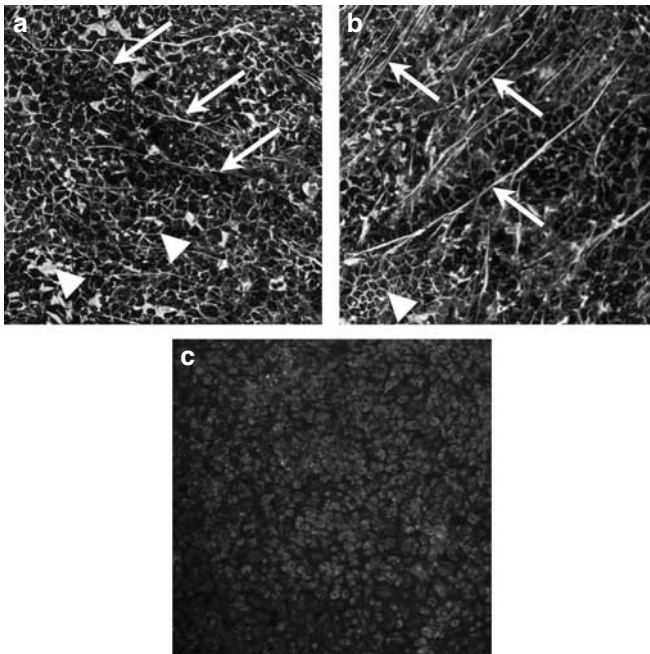


Figure 1 | Expression of HA on HK2 cells. Confluent monolayers of HK2 cells were either (a) serum-deprived for 48 h or (b) grown in the presence of 2% (v/v) FCS before fixation with methanol and detection of HA by addition of bHABP. Sections were imaged by confocal microscopy ($\times 10$ objective). To confirm the nature of HA staining, in parallel experiments, cells were treated with (c) bovine testicular hyaluronidase (final concentration 200 μ g/ml) at 37°C for 5 min, before fixation and addition of biotinylated HA-binding protein. Pericellular coats are highlighted by arrowheads and HA cables by white arrows. Original magnification $\times 10$.

Role of I α I in cable formation. We used a commercial antibody, which recognizes all components of I α I (HC1, HC2, and bikunin) and intact P α I, to examine the localization of one or more of these proteins in HA cables. Using this antibody, confocal microscopy of HK2 cells, serum deprived for 48 h, revealed colocalization with the HA cables (Figure 2). This suggests that components of the I α I family are incorporated into the HA cables.

Incubation of cells under serum-free conditions in the presence of the I α I/P α I antibody resulted in severe truncation of the HA cables, and at the higher antibody concentration, there was complete absence of HA cable formation (Figure 3). The effect of the antibody could be overcome by the addition of the antibody in the presence of 2% (w/v) FCS, a source of I α I and P α I. Under these conditions, it is likely that serum-derived HCs are in excess, and thus overcome the inhibitory action of the antibody.

Previously, we demonstrated that monocyte binding is mediated by HA cables.¹⁰ Having demonstrated reduced cable formation in the presence of antibody to I α I/P α I in parallel experiments, we subsequently examined the effect of the antibody on adhesion of U937 cells to HK2 cells. Reduction of HA cable formation by antibody to I α I was accompanied by significant attenuation of monocyte binding (Figure 4).

Inhibition of TSG-6. Studies utilizing the Tsg-6^{-/-} mouse have demonstrated that TSG-6 is critical in the formation of stable HA matrices.¹⁵ In the current study, we were unable to demonstrate colocalization of TSG-6 and HA cables by confocal microscopy. Incubation of HK2 cells with anti-TSG-6 monoclonal antibody A38, previously demonstrated to block HA binding to TSG-6²² and to inhibit the formation of TSG-6·HC complexes *in vitro*,²³ did not influence cable formation (data not shown), and had no effect on

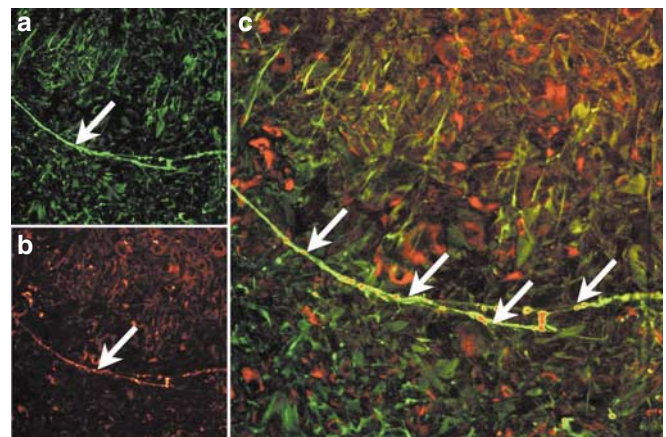


Figure 2 | Localization of I α I/P α I. HK2 cells were grown to confluence in the presence of 10% (v/v) FCS, before fixation with methanol. (a) HA was detected by bHABP and fluorescent avidin-D, and (b) I α I/P α I detected by addition of polyclonal antibody to I α I/P α I (dilution 1:100) and Alexa Flour 568 conjugate. (c) Colocalization of HA and I α I/P α I was examined by merging of individual images. HA cables are highlighted by arrows. Original magnification $\times 10$.

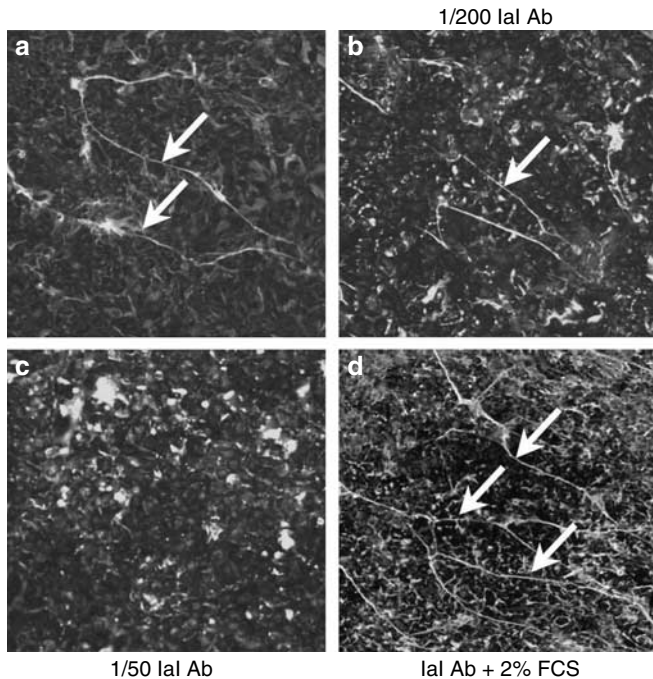


Figure 3 | Incubation with antibody to I α 1/P α 1 inhibits cable formation. Confluent monolayers of HK2 cells were incubated (a) in serum-free medium or serum-free medium to which polyclonal antibody to I α 1/P α 1 had been added at a final dilution of either (b) 1:200 or (c) 1:50 for 24 h before fixation with methanol. HA was detected using bHABP as before and sections imaged by confocal microscopy ($\times 10$ objective). (d) In addition, confluent monolayers of cells were incubated with the polyclonal I α 1/P α 1 antibody in the presence of 2% (v/v) FCS for 24 h before fixation and visualization of HA. Pericellular coats are highlighted by arrowheads and HA cables by white arrows.

HA-dependent monocyte binding to monolayers of HK2 cells (Figure 5).

Versican is a component of HA cables. Previous work demonstrated colocalization of versican, a large chondroitin sulfate proteoglycan and hyaladherin with HA in cables in smooth muscle cells.²⁴ Confocal microscopy confirmed localization of versican into HA cables in our epithelial cell system (Figure 5).

HAS3 overexpression

Generation of a stable cell line and characterization of altered HA synthesis. HA generation by the cell lines was examined both by enzyme-linked immunosorbent assay of the cell culture supernatant and also following [3 H]glucosamine labelling of HA (Figure 6a–c). Confluent monolayers of HAS3-expressing cells or mock-transfected cells were serum deprived for 48 h. Fresh serum-free medium was subsequently added, for a further 24 h before collection, and HA quantified by enzyme-linked immunosorbent assay (Figure 6d). HA concentration in the culture supernatant was significantly greater in the HAS3-expressing cell line. This represented a 32% increase in the HA over the mock-transfected cells ($P=0.004$). Increased HAS3 mRNA expres-

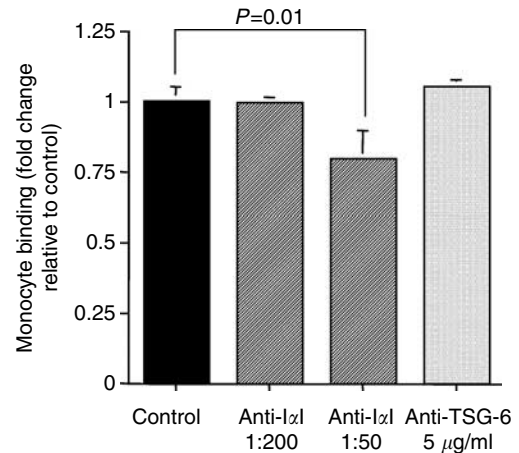


Figure 4 | Monocyte binding is decreased by inhibition of cable formation. Confluent monolayers of HK2 cells were incubated with polyclonal antibody to I α 1/P α 1 or A38 monoclonal antibody to TSG-6 (5 μ g/ml) for 24 h. Subsequently, the monolayer was washed with PBS before the addition of 1×10^6 51 Cr-labelled U937 cells again under serum-free conditions for 1 h at 37°C. Quantitation of bound radioactivity was carried out as described in Materials and Methods. Data represent mean \pm s.d., $n=3$.

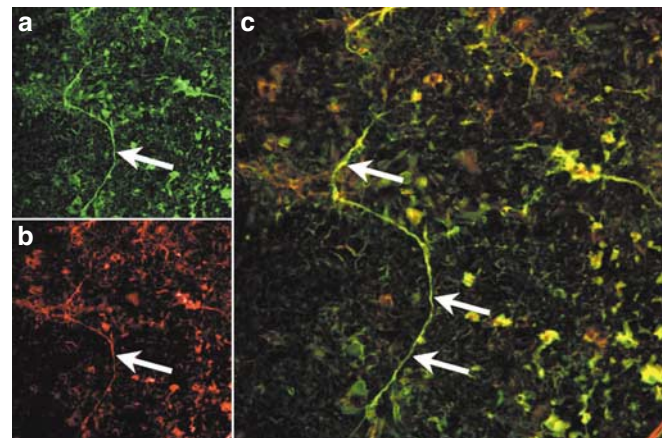


Figure 5 | Localization of versican. HK2 cells were grown to confluence in the presence of 10% (v/v) FCS, and serum deprived for 48 h before fixation with methanol. (a) HA was detected by addition of bHABP and fluorescent avidin-D, and (b) versican detected by addition of monoclonal antibody to versican (clone 2B1) and Alexa Flour 568-conjugated antibody. (c) Colocalization of HA and versican was examined by merging of individual images. HA cables are highlighted by arrows. Original magnification $\times 10$.

sion in the transfected cells was confirmed by reverse transcription-polymerase chain reaction (PCR) (Figure 6e).

Analysis on Sephacryl S-500 of the [3 H]glucosamine-labelled HA samples from both the HAS3-overexpressing cell line and the mock-transfected cells demonstrated that the majority of the labelled HA in the supernatant and the trypsin extracts appeared near the void volume and therefore was considered to be of high molecular mass (Figure 6a and b). In addition, there was a marked increase in the generation of medium and low molecular weight HA in the supernatant of the HAS3-overexpressing cells as compared to the

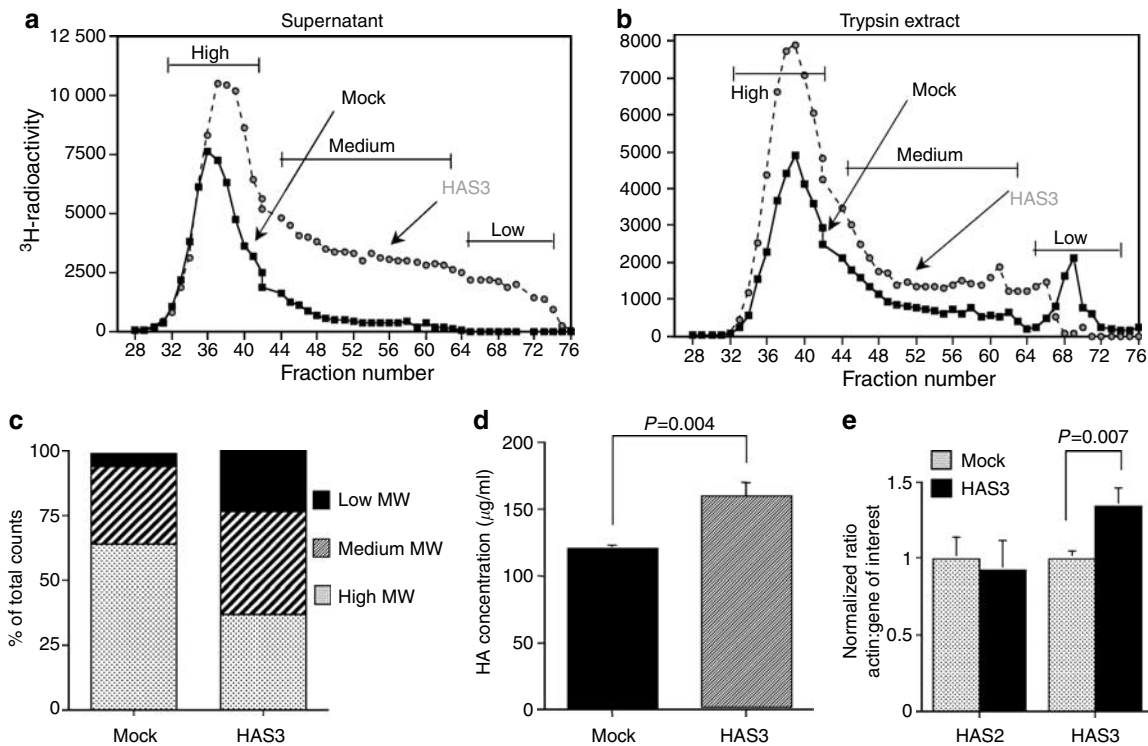


Figure 6 | HAS3 overexpression and characterization of HA. Confluent serum deprived monolayers of HAS3-overexpressing cells (open circles) or mock-transfected cells (boxes) were exposed to serum-free conditions for 24 h in the presence of 20 $\mu\text{Ci/ml}$ [^3H]glucosamine. (a) Supernatant and (b) trypsin extracts were prepared as described in Materials and Methods. Radiolabelled HA was subsequently analyzed by Sephacryl S-500 chromatography. (c) Subsequently, the distribution of HA between high ($> 10^6$ Da), medium (10^5 – 10^6 Da), and low ($< 10^5$ Da) molecular weight fraction for the mock-transfected and HAS3 cell lines were calculated and the data presented as the percentage of the total of HA in each molecular weight fraction. (d) In a parallel experiment, supernatant samples were collected from confluent serum-deprived mock-transfected and HAS3-overexpressing cells and HA quantified by enzyme-linked immunosorbent assay. In addition, the relative expression levels of HAS2 and HAS3 mRNA expression in the mock-transfected and HAS3-overexpressing cells were examined by reverse transcription-PCR. Total mRNA was extracted from confluent monolayers of mock-transfected and HAS3-overexpressing cells after 48 h of serum deprivations. PCR products were separated on a 3% (w/v) agarose gel and stained with ethidium bromide. PCR amplification was carried out for 28 cycles for β -actin mRNA, 32 cycles for HAS2 mRNA, and 36 cycles for HAS3 mRNA. Densitometric ratios of the gene of interest compared to the housekeeping gene β -actin normalized to the ratio seen in the mock-transfected cells of three individual experiments are shown with the data representing mean \pm s.d.

mock-transfected cells. The medium and low molecular weight fractions for mock-transfected cells represent 35% of the total compared to 62% in the HAS3 cells.

The increased HA in the trypsin extract of the HAS3-overexpressing cells is suggestive of increased protein-bound cell-associated HA previously shown to be anchored by CD44.²⁵ Previously, we have shown reduced cell surface expression of CD44 in a HAS2-overexpressing cell line. In contrast, the HAS3 cell line cell-surface CD44 expression increased as assessed by flow cytometry (Figure 7).

Visualization of HA. As with untransfected cells, confocal imaging was used to examine the organization of HA on the cell surface. These images demonstrated a marked increase in HA, both in pericellular coats and also in HA cables, in the HAS3-overexpressing cells as compared to mock-transfected cells (Figure 8). Limited hyaluronidase digestion removed both of these pericellular structures confirming the HA content (data not shown).

Functional alterations associated with HAS3 overexpression. Cell migration was assessed in a previously characterized

scratch wound system.^{6,26} Confluent monolayers of cells were serum deprived for 48 h before generation of an intersecting area of denuded cells by scraping with a sterile 1000 μl pipette tip. Closure of the denuded area was then monitored at different times. At all time points beyond 24 h, the number of migrating cells entering the ‘denuded area’ was significantly greater in the HAS3-overexpressing cells compared to the mock-transfected cells (Figure 9a). To demonstrate that increased migration was dependent on altered HA generation, the HAS3-overexpressing cells were subjected to limited hyaluronidase digestion following generation of the ‘denuded area’. Removal of pericellular HA using this method significantly attenuated the migratory response of the HAS3-overexpressing cells (Figure 9a).

Consistent with the increase in HA cable formation, monocyte binding by the HAS3-overexpressing cells was increased. Treatment of the monolayer with hyaluronidase significantly reduced monocyte binding, confirming its dependence on cell-associated HA (Figure 9b).

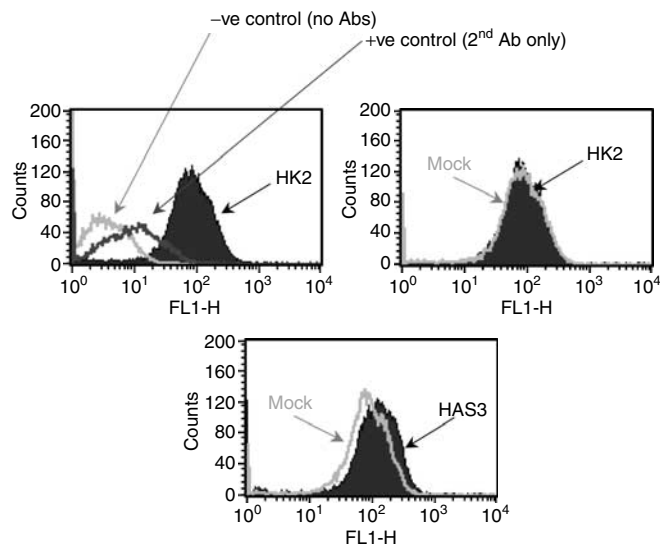


Figure 7 | Confluent monolayers of HK2 cells, mock or HAS3-overexpressing cells were serum deprived for 48 h before detachment. Cells were incubated with anti-CD44 common region antibody, and cell surface expression of CD44 was assessed by FACS analysis.

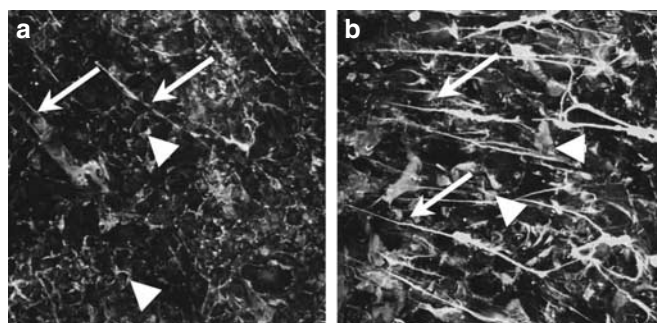


Figure 8 | Visualization of HA in HAS3-overexpressing cells. Confluent monolayers of (a) mock-transfected and (b) HAS3-overexpressing cells were serum deprived for 48 h before fixation with methanol and detection of HA by the addition of bHABP. Sections were imaged by confocal microscopy ($\times 10$ objective). Pericellular coats are highlighted by arrowheads and HA cables by white arrows. Original magnification $\times 20$.

Reverse transcription-PCR. HAS3 overexpression was associated with significant induction of *hyal1* and *hyal2* mRNA. In contrast to the previous report in HAS2-overexpressing cells,²¹ in the HAS3 transfectants, *PxI HC3* mRNA was not suppressed and *bikunin* mRNA was significantly increased (Figure 10).

DISCUSSION

Several cell types *in vitro* surround themselves with HA in an organized pericellular matrix or ‘coat’,^{27,28} in which HA may be anchored to the surface of cells via an interaction with CD44.²⁵ In PTCs, increased assembly of HA into pericellular coats is associated with a migratory phenotype.²¹ As migration of PTCs has been identified as one of the

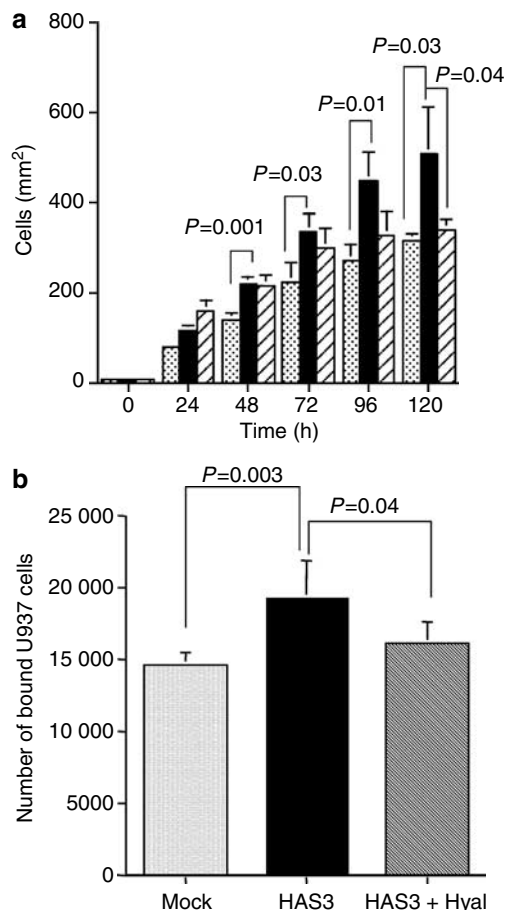


Figure 9 | Alterations in cell function associated with HAS3 overexpression. (a) Quantification of cell migration. Confluent serum-deprived monolayers of mock- (stippled bars) or HAS3-overexpressing cells (solid bars) were scratched as described in Materials and Methods to produce an intersecting area denuded of cells. In addition, for HAS3-overexpressing cells, to confirm the role of HA, following generation of a denuded area, cells were treated with bovine testicular hyaluronidase (final concentration 200 $\mu\text{g}/\text{ml}$) at 37°C for 5 min (cross-hatched bars). Subsequently, following washing of the monolayer to remove detached cells, the rate of cell migration of each was assessed by directly counting the number of cells migrating into the intersecting denuded area at each of the time points indicated. The data are expressed as the number of cells per mm^2 of denuded area. Data represent the mean \pm s.d. of four individual experiments. (b) Quantitation of monocyte binding. Confluent monolayers of mock-transfected or HAS3-overexpressing cells were washed with PBS before the addition of 1×10^6 ^{51}Cr -labelled U937 cells again under serum-free conditions for 1 h at 37°C. Quantitation of bound radioactivity was carried out as described in Materials and Methods. To quantify HA-dependent binding, the monolayer of HAS3-overexpressing cells was treated with bovine testicular hyaluronidase (H’ase) (final concentration 200 $\mu\text{g}/\text{ml}$) at 37°C for 5 min before the addition of monocytes. Data represent mean \pm s.d. of six individual experiments.

important steps of epithelial cell transdifferentiation,²⁹ in the context of progressive renal disease, an increase in pericellular HA may therefore facilitate the fibrotic response.

Recently, in addition to pericellular HA ‘coats’, we have demonstrated that PTCs form pericellular HA cable-like structures that support interactions with monocytes via their

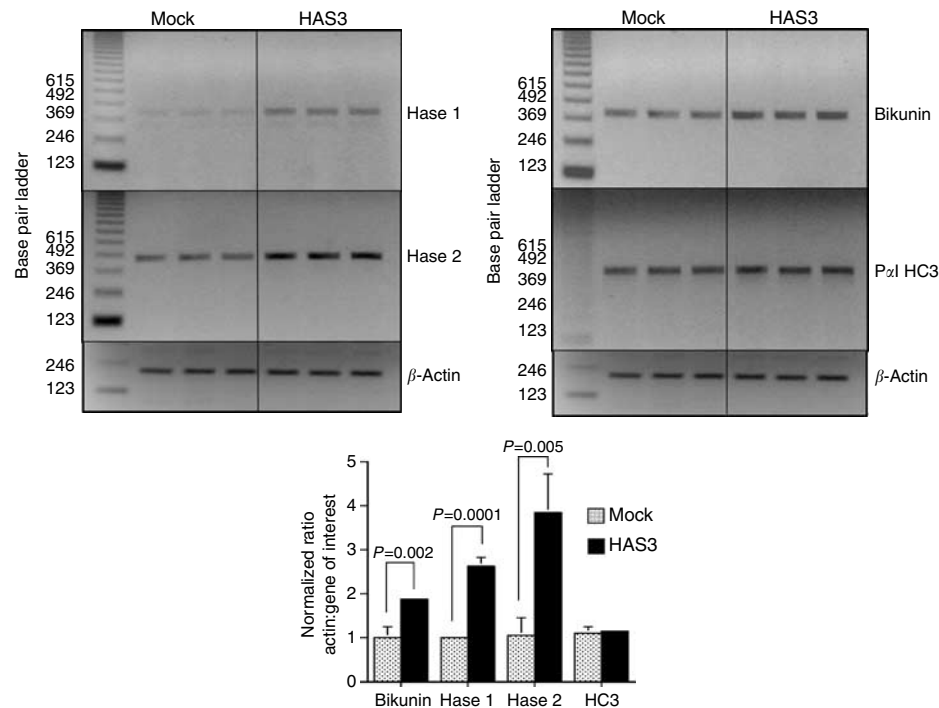


Figure 10 | Total mRNA was extracted from confluent monolayers of mock-transfected and HAS3-overexpressing cells after 48 h of serum deprivation. PCR products were separated on a 3% (w/v) agarose gel and stained with ethidium bromide. For each gene of interest, three representative PCR reactions are shown. PCR amplification was carried out for 28 cycles for β -actin mRNA, 36 cycles for hyal1 mRNA, 32 cycles for hyal2 mRNA, 36 cycles for P α I HC3 mRNA, and 36 cycles for bikunin. Densitometric ratios of the gene of interest compared to the housekeeping gene β -actin of three individual experiments are shown with the data representing mean \pm s.d.

cell-surface CD44 receptors,¹⁰ masking cell-surface interactions that drive intercellular adhesion molecule-dependent TGF- β 1 generation.^{30,31} Inflammatory cell infiltrate, and particularly monocyte/macrophage infiltrate, has been implicated in the pathogenesis of a wide diversity of renal diseases.^{32–34} Understanding the mechanism by which HA mediates inflammatory cell recruitment and its regulation, therefore, has important relevance to kidney disease and our data would suggest that synthesis of HA cables may limit renal fibrosis. Consistent with this hypothesis is our observation that cable formation is stimulated by bone morphogenic protein-7.¹⁰ Bone morphogenic protein-7-stimulated cable formation was associated with downregulation of hyaluronidase expression. More recently, we have shown that decreased HA cable formation in HAS2-overexpressing cells was associated with an increase in hyaluronidase expression. This led us to postulate that hyaluronidase expression may be causally related to HA cable formation. The data in the current study would suggest that this is not the case, as increased HA cable formation in the HAS3-overexpressing cells occurred despite the increase in hyaluronidase activity. The increase in hyaluronidase expression in both the HAS2- and HAS3-overexpressing cells therefore more likely represents a feedback response of the cell when it encounters an excess of HA, which is not causally related to the absence of cables in HAS2-overexpressing cells.

The data demonstrate the incorporation of components of the I α I family of proteins into the HA cables and suggests that they are important in cable assembly. Both cable assembly and HA-dependent monocyte binding in PTCs was inhibited by antibody to I α I/P α I. Although, as with colonic smooth muscle cell in which HA cables were first described, addition of serum enhanced cable formation, in PTC HA cables are formed in the absence of serum. We have previously demonstrated that PTCs generate the P α I variant of the I α I family.¹² This may therefore explain the generation of cables by PTCs in the absence of serum, which is the source of I α I family protein components for colonic smooth muscle cells. This hypothesis is further supported by the demonstration of HA cables in the HAS3-overexpressing cell line, in contrast to reduced HA cable formation previously seen in an HAS2-overexpressing cell line,²¹ as one difference between the two cell lines is the expression of HC3 mRNA, which is markedly downregulated in the HAS2 cells while abundantly expressed in the HAS3 cells.

TSG-6 is an inflammation-associated, secreted protein composed of contiguous link module and CUB domains. It can bind to HA directly through its link module^{35,36} and has also been demonstrated to play an important role in the transfer of HCs from I α I/P α I onto HA;^{15,37} this reaction can be visualized in a cell-free system utilizing purified I α I, HA, and TSG-6 in the absence of serum. Its role in transfer of HC3 from P α I is less well understood. In an *in vitro* assay in

the absence of serum, TSG-6 does not support the transfer of HC3 from P α I to HA,³⁷ although studies in the *Tsg-6*^{-/-} mouse,¹⁵ or the use of serum as a source of this protein,³⁷ do suggest that TSG-6 *in vivo* is involved in HC3 transfer. Previously, we have demonstrated that the transfer of HCs of I α I/P α I to HA by TSG-6 is involved in the formation of pericellular HA coats.²¹ In contrast, the data presented in the current study suggest that TSG-6 is not such a key player in the incorporation of I α I/P α I components into the HA cables. This observation that TSG-6 is not a critical factor in the formation of HA cables is also consistent with our previous published observations, which demonstrate that interleukin-1 β stimulates PTC TSG-6 synthesis,¹² but decreases the formation of HA cables and HA-dependent monocyte binding,¹⁰ despite being a potent stimulus of PTC HA generation.²⁰ From these data, we propose that upregulation of TSG-6 during inflammation may represent a harmful process stimulating a migratory phenotype in the PTCs, and suppressing the formation of HA cables, which may in turn suppress the anti-inflammatory effect of HA cables on infiltrating inflammatory cells. However, this is perhaps surprising given the anti-inflammatory properties of TSG-6 determined in other tissues.^{38,39}

Another hyaladherin that we have identified as a component of HA cables is the large chondroitin sulfate proteoglycan versican. Data generated using colonic smooth muscle cells suggested that it is important in binding leukocytes to cables, although the counter-receptor on the leukocyte has not been fully characterized.²⁴ Its role in cable assembly, however, is not well understood. Interleukin-1 β , which abrogates PTC cable formation, in other cell systems is a known inhibitor of versican synthesis,⁴⁰ and we have demonstrated it to be a potent stimulator of TSG-6 synthesis in PTCs.¹² Interestingly, chondroitin-4-sulfate competes efficiently for HA binding to the TSG-6 link module.¹⁸ Wisniewski *et al.*⁴¹ have recently confirmed that chondroitin-4-sulfate is an effective inhibitor of HA binding to full-length TSG-6. TSG-6 link module also binds to the G1 domain of human versican (VG1). Versican has also been shown to bind HCs of the I α I family⁴² and supports the transfer of HCs onto HA.¹³ This raises the possibility that TSG-6-versican counter-regulatory mechanisms exist that modulate HA-matrix assembly, altering the balance between HA coat and cable formation. In addition to its structural role in HA cables, it is therefore interesting to speculate that induction of versican may result in the abrogation of TSG-6 HC transfer activity, hampering coat formation and favoring cable assembly. This role for versican, in the assembly of HA cables, is also consistent with studies demonstrating an anti-inflammatory effect for versican that can bind specific chemokines, which inhibits chemokine function.⁴³

In summary, the data suggest that regulation of hyaladherins in the face of constitutive HA generation, may be the key to cable assembly rather than induction of HA synthesis *per se*.

MATERIALS AND METHODS

Cell culture

All experiments were carried out using HK2 cells (American Type Culture Collection Number CRL-2190), which are human PTCs immortalized by transduction with human papilloma virus 16 E6/E7 genes⁴⁴ as described previously.¹⁰ Cell migration was examined as described previously.^{45,46} Briefly, to quantify re-epithelialization, an intersecting area of denuded cells was generated, and closure of the denuded area monitored using an Axiovert 100M inverted microscope fitted with a digital camera (ORCA-1394, Hamamatsu Photonics KK Hamamatsu, Japan).

U937 cells, originally derived from a human histiocytic lymphoma, were procured from the American Type Culture Collection (Rockville, MD, USA). The cells were grown in suspension culture in Roswell Park Memorial Institute (RPMI) medium supplemented with L-glutamine and penicillin/streptomycin, and containing 5% (v/v) fetal bovine serum.

Immunocytochemistry

For immunocytochemistry, cells were fixed by the addition of 100% ice-cold methanol for 15 min at -20°C. For HA staining, a biotinylated HA-binding protein (bHABP (Seikagaku Corporation, Tokyo, Japan)) was then added (5 μ g/ml) and incubated at 4°C overnight. Rabbit polyclonal antibody to I α I (Dako Cytomation Ltd, Cambridge, UK), monoclonal anti-human large proteoglycan (clone 2-B-1, Seikagaku), and polyclonal rabbit-anti-human TSG-6 antibody (RAH-1) were used for the detection of I α I/P α I, versican, and TSG-6, respectively. The slides were washed with phosphate-buffered saline (PBS) before incubation with either fluorescent avidin-D (20 μ g/ml) for the detection of HA (Vector Laboratories, Burlingame, CA, USA) or with appropriate AlexaFlour 568-conjugated antibody (10 μ g/ml) (Cambridge Bioscience, Ely, UK) for the detection of I α I or versican, at room temperature for 1 h. Following a final washing step, specimens were affixed to the slides in Vectashield mounting medium (Vector Laboratories), and analyzed by confocal laser scanning microscopy (TCS-40 Leica Microsystems, Cambridge, UK).

Assay for leukocyte adhesion

U937 cell adhesion was measured as described previously.⁴⁷ Confluent HK2 cells were serum deprived for 48 h before the leukocyte adhesion assay. Subsequently, the medium was removed from HK2 cultures, and 10⁶ μ ⁵¹Cr- (as sodium chromate, Amersham BioSciences, Chalford St Giles, UK) labelled U937 cells added to each well. The binding phase of the assay was carried out at 4°C for 1 h. All cultures were washed with cold medium before lysis by 1% (v/v) Triton X-100. An aliquot was subsequently removed for quantification of radiolabel. The number of the U937 cells bound per well was calculated from the initial specific activity (cpm/cell). Spontaneous release of chromium from U937 cells in control incubations without HK2 cells was typically less than 10%.

Generation of HAS3-overexpressing clone

The HAS3 ORF (gift from Andrew Spicer) was extracted from a pCI-neo expression vector by restriction enzyme digestion (*Xba*I and *Xho*I) and inserted into a pcDNA4/TO vector (Invitrogen, Carlsbad, CA, USA), using a standard ligation reaction with Promega Ligase enzyme. Amplification of the cloned vector was carried out via bacterial transformation (JM109-competent *Escherichia coli* – Promega, Madison, WI, USA). The integrity of the HAS3

ORF was confirmed by restriction enzyme (*Xba*I and *Xho*I) digestion (Figure 1) and sequencing (data not shown).

To establish stable transfection, sub-confluent HK2 cells in 35 mm Petri dishes were transfected with either HAS3-pcDNA4/TO or pcDNA4/TO empty vector (Mock) using FuGENE 6 Transfection Reagent (from Roche Diagnostics, Indianapolis, IN, USA) under serum-free conditions. Transfected cells were selected using the Zeocin-resistant gene present in the pcDNA4/TO vector. The transfection mixture contained 3 μ l of FuGENE 6 and 1 μ g of vector DNA. After 24 h of transfection, 400 μ g/ml of Zeocin Antibiotic (Invitrogen Life Technologies) was added to each plate. Culture media (with Zeocin) were changed afterwards every 3–4 days until distinct colonies were observed in the plates at about 14 days post-transfection. For each transfection, all of the colonies were trypsinized and combined to give stable cell pools. Transfected cells were maintained in the presence of 200 μ g/ml of Zeocin.

Alteration in mRNA expression

The expression of mRNAs for the HA synthases, the hyaluronidases, and bikunin and HC3 from *P α I* were determined by reverse transcription-PCR using specific oligonucleotide primers (Table 1) as described previously.⁴⁸ PCR was carried out for various cycles (28–40 cycles), to ensure that amplification was in the linear range of the curve. Following PCR, samples were separated by flat bed electrophoresis in 3% (w/v) NuSieve GTG agarose gels (Flowgen Instruments Ltd, Sittingbourne, UK) and stained with ethidium bromide (Sigma-Aldrich, Gillingham, UK). Results were expressed as the ratio of the gene of interest to that of β -actin, normalized to the control value (the ratio in the unstimulated cells) of each experiment.

Flow cytometry

Cell surface expression of CD44 was assessed by fluorescence-activated cell sorting (FACS) analysis. Following detachment of HK2 cell monolayers, the cells were incubated with anti-CD44 common region antibody (Calbiochem, San Diego, CA, USA) for 30 min at 4°C (antibody dilution 1:500). FITC-labelled secondary antibody (Sigma, dilution 1:100) was then added in FACS buffer (PBS, 10 mM ethylenediaminetetraacetic acid (Sigma-Aldrich), 15 mM sodium azide (Fisher Chemicals, Loughborough, UK), and 5% (w/v) bovine serum albumin (Sigma-Aldrich), pH 7.35) for 30 min at 4°C. In control experiments, secondary antibody only was added to the cells. After three washes in FACS buffer, the data were collected using a

Becton Dickinson FACSCalibur 4CaTM, and analyzed using CellQuest ProTM software.

Analysis of ³H-radiolabelled HA

Confluent monolayers of cells were serum deprived for 48 h before *in vitro* ³H-labelling of HA with [³H]glucosamine under serum-free conditions for 72 h as described previously.⁴⁹ Supernatant samples were collected and treated with equal volumes of 200 μ g/ml pronase (Sigma-Aldrich) for 24 h at 37°C to analyze HA released into the culture medium (Supernatant). The remaining cell monolayers were incubated with 10 μ g/ml trypsin (Sigma-Aldrich) in PBS for 10 min at room temperature to remove pericellular (protein-bound) ³H-HA (Trypsin Extract) before the addition of an equal volume of 100 μ g/ml pronase for 24 h at 37°C.

Each of the fractions was subsequently passed over diethylamino ethanol (DEAE) ion-exchange columns (Amersham Biosciences) equilibrated with 8 M urea (pH 6) in Bis-Tris buffer. The columns were washed using 8 M urea buffer to remove low molecular weight peptides and unincorporated radiolabel. HA was then eluted with 0.3 M NaCl in the urea buffer. Equal volumes of eluted HA were then precipitated by three volumes of 1.3% (w/v) potassium acetate in 95% (v/v) ethanol in the presence of 50 μ g/ml of each glycosaminoglycan: HA, heparin (Sigma-Aldrich) and chondroitin sulfate (Sigma-Aldrich) as co-precipitants. Precipitated HA from two equal volumes were either dissolved in 4 M guanidine HCl buffer or incubated with 1 IU streptococcal hyaluronidase (ICN Biomedicals, Basingstoke, UK) at 37°C for 24 h before the addition of equal volumes of 8 M guanidine HCl buffer (pH 6). Each sample was run through a Sephacryl S-500 column (Amersham Biosciences) and eluted with 4 M guanidine HCl buffer before quantitation of radioactivity in the eluted fractions. The value of the hyaluronidase-treated portion subtracted from the non-hyaluronidase-treated portion was taken as ³H-associated radioactivity in HA.

Statistical analysis

Statistical analysis was carried out using the unpaired Student's *t*-test, with a value of *P* < 0.05 considered to represent a significant difference. The data are presented as means \pm s.d. of *n* experiments. For each individual experiment, the mean of duplicate determinations was calculated.

ACKNOWLEDGMENTS

This work was supported in part by a research grant from the Diabetes UK. AOP is supported by a GlaxoSmithKline Advanced Fellowship. The Institute of Nephrology is supported by Kidney Wales Foundation. AJD acknowledges the support of the Arthritis Research Campaign (Grants 16119 and 16539) and the Medical Research Council.

REFERENCES

- Hansell P, Göransson V, Odland C *et al.* Hyaluronan content in the kidney in different states of body hydration. *Kidney Int* 2000; **58**: 2061–2068.
- Sibalic V, Fan X, Loffing J *et al.* Upregulated renal tubular CD44, hyaluronan, and osteopontin in kd kd mice with interstitial nephritis. *Nephrol Dial Transplant* 1997; **12**: 1344–1353.
- Lewington AJP, Padanilam BJ, Martin DR *et al.* Expression of CD44 in kidney after acute ischemic injury in rats. *Am J Physiol* 2000; **278**: R247–R254.
- Wells A, Larsson E, Hanas E *et al.* Increased hyaluronan in acutely rejecting human kidney grafts. *Transplantation* 1993; **55**: 1346–1349.
- Wells AF, Larsson E, Tengblad A *et al.* The localisation of hyaluronan in normal and rejected human kidneys. *Transplantation* 1990; **50**: 240–243.
- Ito T, Williams JD, Al-Assaf S *et al.* Hyaluronan and proximal tubular epithelial cell migration. *Kidney Int* 2004; **65**: 823–833.

Table 1 | Sequence of oligonucleotide primers

Gene	Primer sequence	Product size (bp)
β -Actin	F=5'-CCTTCTGGGCATGGAGTCCT-3' R=5'-GGAGCAATGATCTTGATCTT-3'	204
HAS2	F=5'-GCAGGCGGAAGAAGGGACAAC-3' R=5'-TCAGGCGGATGCACAGTAAGGA-3'	313
HAS3	F=5'-AGTGCAGCTTCGGGGATGA-3' R=5'-TGATGGTAGCAATGGCAAAGAT-3'	453
hyal1	F=5'- CAGGCGTGAGCTGGATGGAGA-3' R=5'- GTATGTGCAACACCGTGTGGC-3'	400
hyal2	F=5'- GAGTTCGCAGCACAGCAGTTC-3' R=5'- CACCCAGAGGATGACACCAG-3'	446
Pal HC3	F=5'-AGTACCCCGAGAACGCTATCCTG-3' R=5'-TGGCCCTCTATCCTCGTTGTCC-3'	411
Bikunin	F=5'-CGTTGGCGGAAAGGTGTCTGTG-3' R=5'-ACCCCTGATCCTTCTTCT-3'	399

HAS2, hyaluronan synthase 2.

7. Ito T, Williams JD, Fraser DJ *et al.* Hyaluronan attenuates TGF- β 1 mediated signalling in renal proximal tubular epithelial cells. *Am J Pathol* 2004; **164**: 1978–1988.
8. Ito T, Williams JD, Fraser DJ *et al.* Hyaluronan regulates TGF- β 1 receptor compartmentalisation. *J Biol Chem* 2004; **279**: 25326–25332.
9. Zhang XL, Topley N, Ito T *et al.* IL-6 regulation of TGF- β receptor compartmentalisation and turnover enhances TGF- β 1 signalling. *J Biol Chem* 2005; **280**: 12239–12245.
10. Selbi WD, De La Motte CA, Hascall VC *et al.* BMP-7 modulates HA mediated proximal tubular cell-monocyte interaction. *J Am Soc Nephrol* 2004; **15**: 1199–1211.
11. Salier JP, Rouet P, Raguenes G *et al.* The inter-alpha inhibitor: from structure to regulation. *Biochem J* 1996; **315**: 1–9.
12. Janssen U, Thomas G, Glant T *et al.* Regulation of inter-alpha-trypsin inhibitor (Ial) and tumour necrosis factor-stimulated gene 6 (TSG-6) expression in human renal proximal tubular epithelial cells. *Kidney Int* 2001; **60**: 126–136.
13. Zhuo L, Hascall VC, Kimata K. Inter-alpha-trypsin inhibitor, a covalent protein-glycosaminoglycan-protein complex. *J Biol Chem* 2004; **279**: 38079–38082.
14. Zhuo L, Yoneda M, Zhao M *et al.* Defect in SHAP-hyaluronan complex causes severe female infertility. A study by inactivation of the bikunin gene in mice. *J Biol Chem* 2001; **276**: 7693–7696.
15. Fulop C, Szanto S, Mukhopadhyay D *et al.* Impaired cumulus mucification and female sterility in tumor necrosis factor-induced protein-6 deficient mice. *Development* 2003; **130**: 2253–2261.
16. Kobayashi H, Gotoh J, Hirashima Y *et al.* Inter alpha inhibitor bound to tumour cells is cleaved into the heavy chains and the light chain on the cell surface. *J Biol Chem* 1996; **271**: 11362–11367.
17. Chen L, Mao SJ, McLean LR *et al.* Proteins of the inter-alpha-trypsin inhibitor family stabilize the cumulus extracellular matrix through their direct binding with hyaluronic acid. *J Biol Chem* 1994; **269**: 28282–28287.
18. Parkar AA, Day AJ. Overlapping sites on the link module of human TSG-6 mediate binding to hyaluronan and chondroitin-4-sulphate. *FEBS Lett* 1997; **410**: 413–417.
19. Parkar AA, Kahmann JD, Howat SL *et al.* TSG-6 interacts with hyaluronan and aggrecan in a pH-dependent manner via a common functional element: implications for its regulation in inflamed cartilage. *FEBS Lett* 1998; **428**: 171–176.
20. Jones SG, Jones S, Phillips AO. Regulation of renal proximal tubular epithelial cell hyaluronan generation: implications for diabetic nephropathy. *Kidney Int* 2001; **59**: 1739–1749.
21. Selbi W, Day AJ, Rugg MS *et al.* Over-expression of hyaluronan synthase 2 alters hyaluronan distribution and function in proximal tubular epithelial cells. *J Am Soc Nephrol* 2006; **17**: 1553–1567.
22. Lesley J, English NM, Gal I *et al.* Hyaluronan binding properties of a CD44 chimera containing the link module of TSG-6. *J Biol Chem* 2002; **277**: 26600–26608.
23. Ochsner SA, Day AJ, Rugg MS *et al.* Disrupted function of tumor necrosis factor-alpha-stimulated gene 6 blocks cumulus cell-oocyte complex expansion. *Endocrinology* 2003; **144**: 4376–4384.
24. De La Motte CA, Hascall VC, Drazba J *et al.* Poly I:C induces mononuclear leukocyte-adhesive hyaluronan structures on colon smooth muscle cells: Ialphi and versican facilitate adhesion. In: Kennedy JF, Phillips GO, Williams PA (eds). *Hyaluronan 2000*, vol. 1. Woodhead Publishing Ltd: Wrexham, 2000, pp 381–388.
25. Knudson W, Aguiar DJ, Hua Q *et al.* CD-44 anchored hyaluronan-rich pericellular matrices: an ultrastructural and biochemical analysis. *Exp Cell Res* 1996; **228**: 216–228.
26. Tian YC, Phillips AO. TGF- β 1 mediated inhibition of HK-2 cell migration. *J Am Soc Nephrol* 2003; **14**: 631–640.
27. Evanko SP, Angello JC, Wight TN. Formation of hyaluronan- and versican-rich pericellular matrix is required for proliferation and migration of vascular smooth muscle cells. *Arterioscler Thromb Vasc Biol* 1999; **19**: 1004–1013.
28. Cohen M, Klein E, Geiger B *et al.* Organization and adhesive properties of the hyaluronan pericellular coat of chondrocytes and epithelial cells. *Biophys J* 2003; **85**: 1996–2005.
29. Yang J, Liu Y. Dissection of key events in tubular epithelial to myofibroblast transition and its implications in renal interstitial fibrosis. *Am J Pathol* 2001; **159**: 1465–1475.
30. Zhang XL, Selbi WD, De La Motte CA *et al.* Renal proximal tubular epithelial cells transforming growth factor β 1 generation and monocyte binding. *Am J Pathol* 2004; **165**: 763–773.
31. Zhang XL, Selbi WD, De La Motte CA *et al.* BMP-7 inhibits monocyte stimulated TGF- β 1 generation in renal proximal tubular epithelial cells. *J Am Soc Nephrol* 2005; **1**: 79–89.
32. Young BA, Johnson RJ, Alpers CE *et al.* Cellular events in the evolution of experimental diabetic nephropathy. *Kidney Int* 1995; **47**: 935–944.
33. Lavaud S, Michel O, Sassy-Prigent C *et al.* Early influx of glomerular macrophages precedes glomerulosclerosis in the obese Zucker rat model. *J Am Soc Nephrol* 1996; **7**: 2604–2615.
34. Sassy-Prigent C, Heudes D, Mandet C *et al.* Early glomerular macrophage recruitment in streptozotocin induced diabetic rats. *Diabetes* 2000; **49**: 466–475.
35. Blundell CD, Mahoney DJ, Almond A *et al.* The link module from ovulation- and inflammation-associated protein TSG-6 changes conformation on hyaluronan binding. *J Biol Chem* 2003; **278**: 49261–49270.
36. Lesley J, Gal I, Mahoney DJ *et al.* TSG-6 modulates the interaction between hyaluronan and cell surface CD44. *J Biol Chem* 2004; **279**: 25745–25754.
37. Rugg MS, Willis AC, Mukhopadhyay D *et al.* Characterization of complexes formed between TSG-6 and inter-alpha-inhibitor that act as intermediates in the covalent transfer of heavy chains on to hyaluronan. *J Biol Chem* 2005; **280**: 25674–25686.
38. Bardos T, Kamath RV, Mikecz K *et al.* Anti-inflammatory and chondroprotective effect of TSG-6 in murine models of experimental arthritis. *Am J Pathol* 2001; **159**: 1711–1722.
39. Milner CM, Day AJ. TSG-6: a multifunctional protein associated with inflammation. *J Cell Sci* 2003; **116**: 1863–1873.
40. Qwarnstrom EE, Jarvelainen HT, Kinsella MG *et al.* Interleukin-1 beta regulation of fibroblast proteoglycan synthesis involves a decrease in versican steady-state mRNA levels. *Biochem J* 1993; **294**(Part 2): 613–620.
41. Wisniewski HG, Snitkin ES, Mindrescu C *et al.* TSG-6 protein binding to glycosaminoglycans: formation of stable complexes with hyaluronan and binding to chondroitin sulfates. *J Biol Chem* 2005; **280**: 14476–14484.
42. Eriksen GV, Carlstedt I, Morgelin M *et al.* Isolation and characterization of proteoglycans from human follicular fluid. *Biochem J* 1999; **340**(Part 3): 613–620.
43. Hirose J, Kawashima H, Yoshie O *et al.* Versican interacts with chemokines and modulates cellular responses. *J Biol Chem* 2001; **276**: 5228–5234.
44. Ryan MJ, Johnson G, Kirk J *et al.* HK-2: an immortalized proximal tubule epithelial cell line from normal adult human kidney. *Kidney Int* 1994; **45**: 48–57.
45. Yung S, Davies M. Mechanical injury of human peritoneal mesothelial cells is accompanied by an increase in hyaluronan synthesis. *J Am Soc Nephrol* 1998; **9**: 531.
46. Yung S, Davies M. Response of the human peritoneal mesothelial cell to injury: an *in vitro* model of peritoneal wound healing. *Kidney Int* 1998; **54**: 2160–2169.
47. de la Motte CA, Hascall VC, Calabro A *et al.* Mononuclear leukocytes preferentially bind via CD44 to hyaluronan on human interstitial mucosal smooth muscle cells after virus infection or treatment with poly (I:C). *J Biol Chem* 1999; **274**: 30747–30755.
48. Phillips AO, Steadman R, Topley N *et al.* Elevated D-glucose concentrations modulate TGF- β 1 synthesis by human cultured renal proximal tubular cells: the permissive role of platelet derived growth factor. *Am J Pathol* 1995; **147**: 362–374.
49. Yung S, Thomas GJ, Davies M. Induction of hyaluronan metabolism after mechanical injury of human peritoneal mesothelial cells *in vitro*. *Kidney Int* 2000; **58**: 1953–1962.